JACS
JOURNAL OF THE AMERICAN CHEMICAL SOCIETY
pubs.acs.org/JACS
Article

# High-Pressure Synthesis of Magnetic Neodymium Polyhydrides

Di Zhou, Dmitrii V. Semenok, Hui Xie, Xiaoli Huang,* Defang Duan, Alex Aperis, Peter M. Oppeneer, Michele Galasso, Alexey I. Kartsev, Alexander G. Kvashnin,* Artem R. Oganov,* and Tian Cui*

Cite This: J. Am. Chem. Soc. 2020, 142, 2803−2811
Read Online
ACCESS | Metrics & More | Article Recommendations | Supporting Information

**ABSTRACT:** Ongoing search for room-temperature superconductivity is inspired by the unique properties of the electron−phonon interaction in metal superhydrides. Encouraged by the recently found highest-$T_C$ superconductor *fcc*-$LaH_{10}$, here we discover several superhydrides of another lanthanoid, neodymium. We identify three novel metallic Nd−H phases at pressures ranging from 85 to 135 GPa: *I*4/*mmm*-$NdH_4$, *C*2/*c*-$NdH_7$, and $P6_3/mmc$-$NdH_9$, synthesized by laser-heating metal samples in $NH_3BH_3$ media for in situ generation of hydrogen. A lower trihydride $Fm\bar{3}m$-$NdH_3$ is found at pressures from 2 to 52 GPa. *I*4/*mmm*-$NdH_4$ and *C*2/*c*-$NdH_7$ are stable from 135 to 85 GPa, and $P6_3/mmc$-$NdH_9$ is stable from 110 to 130 GPa. Measurements of the electrical resistance of $NdH_9$ demonstrate a possible superconducting transition at ∼4.5 K in $P6_3/mmc$-$NdH_9$. Our theoretical calculations predict that all of the neodymium hydrides have antiferromagnetic order at pressures below 150 GPa and represent one of the first discovered examples of strongly correlated superhydrides with large exchange spin-splitting in the electronic band structure (>450 meV). The critical Néel temperatures for new neodymium hydrides are estimated using the mean-field approximation to be about 4 K ($NdH_4$), 251 K ($NdH_7$), and 136 K ($NdH_9$).

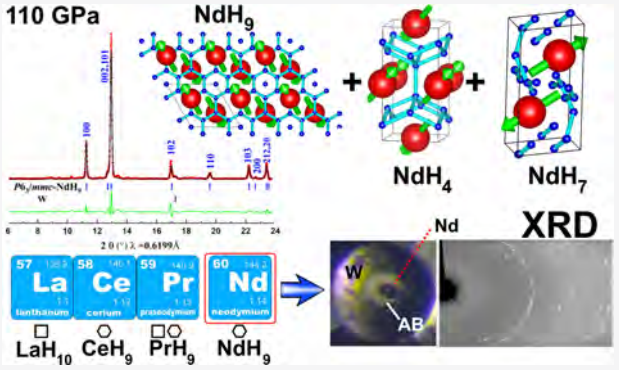


## INTRODUCTION

Since 1968, it is widely discussed that dense metallic hydrogen, if ever produced, could be a high-temperature superconductor.[1] The main reason is its very high Debye temperature (due to low atomic mass) and very strong electron−phonon coupling.[2,3] However, as creating metallic hydrogen requires immense pressures of ∼500 GPa,[4−6] a confirmation of high-$T_C$ superconductivity in pure hydrogen is still pending. Instead, in the search for hydrogen-induced high-temperature superconductivity, most researchers have turned to hydrogen-rich hydrides.[7] Hydrides are promising for high-temperature superconductivity[8−10] under lower pressure as compared to pure metallic hydrogen. Particularly, hydrides are convenient for experimental investigations because of a very high diffusion coefficient of atomic hydrogen, which facilitates the formation of new chemical compounds and makes it possible to perform laser-assisted chemical synthesis in diamond anvil cells in milliseconds.[11]

Just a few years ago, a series of theoretical and experimental studies of various metal hydrides demonstrated that heavy elements relatively easily form metallic superhydrides (i.e., hydrides containing more hydrogen than expected on the basis of atomic valences) at pressures below 200 GPa, such as *fcc*-$LaH_{10}$,[12,13] *P*4/*nmm*-$LaD_{11-12}$,[10] $P6_3/mmc$-$ThH_9$ and $Fm\bar{3}m$-$ThH_{10}$,[14] $P6_3/mmc$-$UH_7$, $Fm\bar{3}m$-$UH_8$,[15] $P6_3/mmc$-$CeH_9$,[16,17] and $P6_3/mmc$- and $F\bar{4}3m$-$PrH_9$,[18] whereas lighter atoms tend to form molecular semiconducting hydrides with low symmetry, for instance, $LiH_6$[19] and $NaH_7$.[20] Extremely high values of $T_C$ have been predicted for $MgH_6$,[21] $CaH_6$,[22] and $YH_{10}$,[23] but these compounds have not been synthesized yet.

One of the most important properties of high-symmetry polyhydrides is a very strong electron−phonon interaction. The critical temperature (>250 K[9,10]) and upper critical magnetic field ($H_C$ up to 140 T) achieved in *fcc*-$LaH_{10}$ have already surpassed by far the parameters of other known compounds, for example, cuprates.[24] Analysis of theoretical results in the field shows that the increasing number of *d*- and *f*-electrons in the electron shells of a hydride-forming atom leads to the enhancement of magnetism, which can suppress superconductivity, and increasing relative contribution of *d*- and *f*-orbitals to the total electron density of states at the Fermi level $N(E_F)$ is associated with weakening of electron−phonon coupling.[25] Thus, the main driver of the study of lanthanoid hydrides is their unusual crystal structures and possible interplay between the classical phonon-mediated superconductivity and magnetic ordering.

Received: October 2, 2019
Published: January 22, 2020







https://dx.doi.org/10.1021/jacs.9b10439
J. Am. Chem. Soc. 2020, 142, 2803−2811

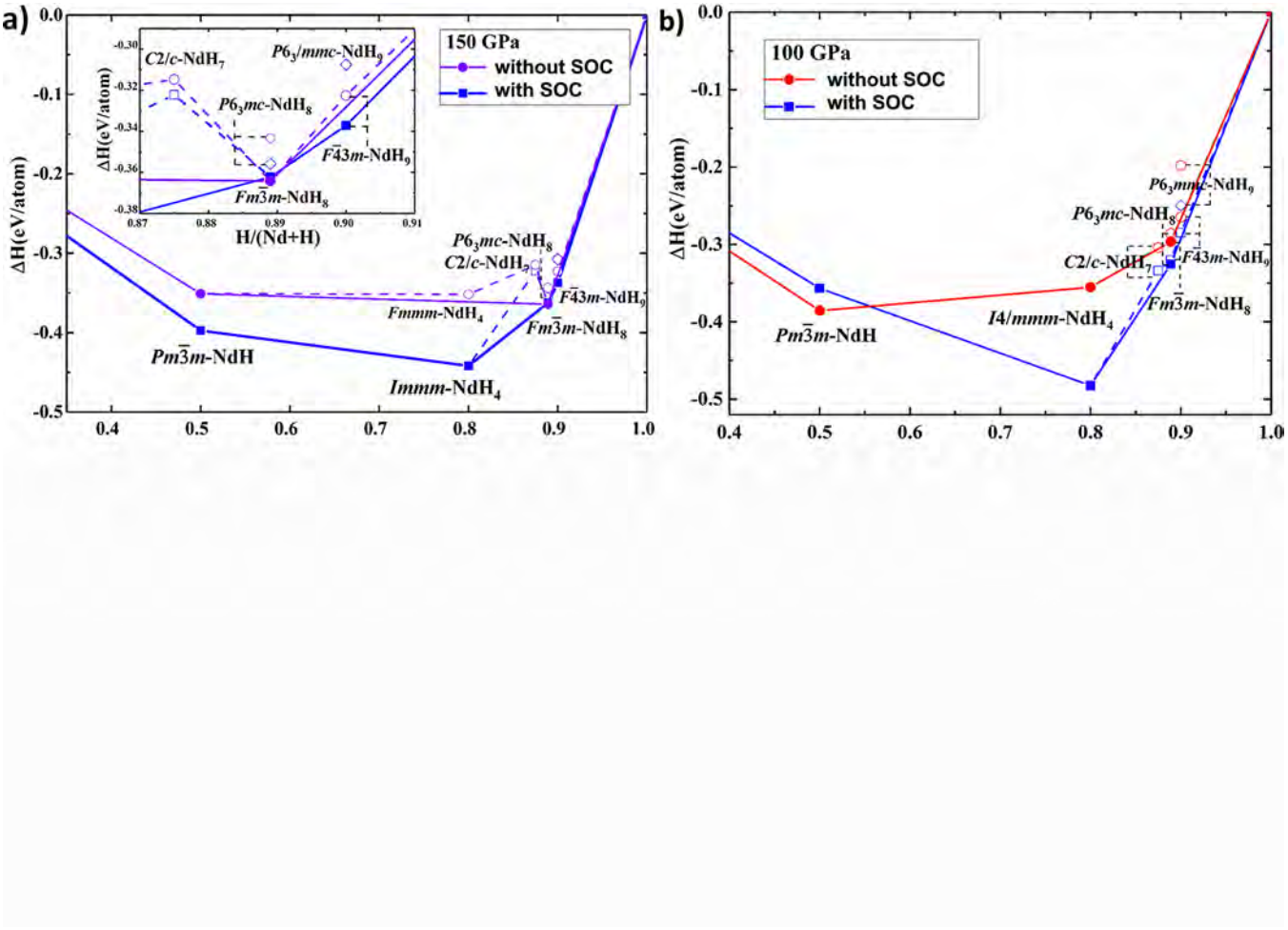


**Figure 1.** Thermodynamic convex hulls of the Nd−H system calculated with and without spin−orbit coupling (SOC) and magnetism at (a) 150 GPa, (b and d) 100 GPa, and (c) 50 GPa. The enlarged part of (b) at 100 GPa is shown in (d).

Currently, high-pressure experimental studies of lanthanoid hydrides are not sufficiently developed, and further investigations of the synthetic pathways and crystal structure of these compounds will contribute to building a deeper understanding of the chemistry and physical properties of metal hydrides. Previously, Chesnut and Vohra[26] studied the crystal structure of metallic Nd at pressures up to 150 GPa and determined the phase sequence occurring as the pressure increases: *dhcp* → *fcc* → *dfcc* (*hR*24) → *hP*3 → monoclinic → *α*-U. Like other lanthanides, Nd can readily absorb hydrogen at high temperatures and form hydrides: $NdH_2$ with cubic close-packed and $NdH_3$ with hexagonal close-packed Nd sublattice were found at ambient pressure.[27] Continuing the investigations of lanthanide−hydrogen systems, we study here the crystal structures and properties of compounds in the Nd−H system in the pressure range of 0−140 GPa. Three novel superhydrides, $NdH_4$, $NdH_7$, and $NdH_9$, are synthesized, which display a fascinating combination of magnetism and superconductivity.

## RESULTS AND DISCUSSION

**Stable Phases Predicted by Theoretical Calculations.** Before the experiment, we carried out several independent variable-composition searches for stable compounds in the Nd−H system at 50, 100, and 150 GPa using the USPEX[28−30] code. The results of the structure search (Figure 1) exhibit large differences depending on the inclusion or exclusion of spin−orbit coupling (SOC) and magnetism. Results with SOC and magnetism indicate that $Pm\bar{3}m$-NdH, tetrahydride *Immm*-$NdH_4$, cubic $Fm\bar{3}m$-$NdH_8$, and $F\bar{4}3m$-$NdH_9$ superhydrides are stable compounds at 150 GPa, while *C*2/*c*-$NdH_7$ lies ∼0.05 eV/atom above the convex hull. $P6_3/mmc$-$NdH_9$, which is similar to recently discovered $CeH_9$ and $PrH_9$, lies 0.035 eV/atom above the convex hull (Figure 1a). At 100 GPa (Figure 1b,d), we see stabilization of the *I*4/*mmm* modification of $NdH_4$ and appearance of $P6_3mc$-$NdH_8$ on the convex hull. At the same time, *C*2/*c*-$NdH_7$ becomes closer (∼0.015 eV/atom) to the convex hull and becomes stable at about 80 GPa. The calculations at 50 GPa without SOC and magnetism show that $P6_3/mmc$-NdH, $P2_1/c$-$NdH_2$, *C*2/*m*-$NdH_3$, and *C*2/*c*-$NdH_7$ are stable (Figure 1c). However, inclusion of spin−orbit coupling leads to dramatic changes in the set of stable phases: $P2_1/c$-$NdH_2$ disappears, while $Fm\bar{3}m$-$NdH_3$ becomes thermodynamically stable. Molecular polyhydride *C*2/*c*-$NdH_7$ maintains its stability at 50 GPa.

**Experimental Synthesis of Atomic *I*4/*mmm*-$NdH_4$ and Molecular *C*2/*c*-$NdH_7$.** The synthesis of neodymium hydrides was performed in a diamond anvil cell (DAC) that we denoted as Z1, containing a piece of Nd compressed in the $NH_3BH_3$ medium to 94 GPa and heated to 1700 K, according to the reaction: Nd + $NH_3BH_3$ → $NdH_x$ + *c*-BN.[31−33] The Raman signal of $H_2$ was detected at 4180.9 $cm^{-1}$, and the


https://dx.doi.org/10.1021/jacs.9b10439
J. Am. Chem. Soc. 2020, 142, 2803−2811

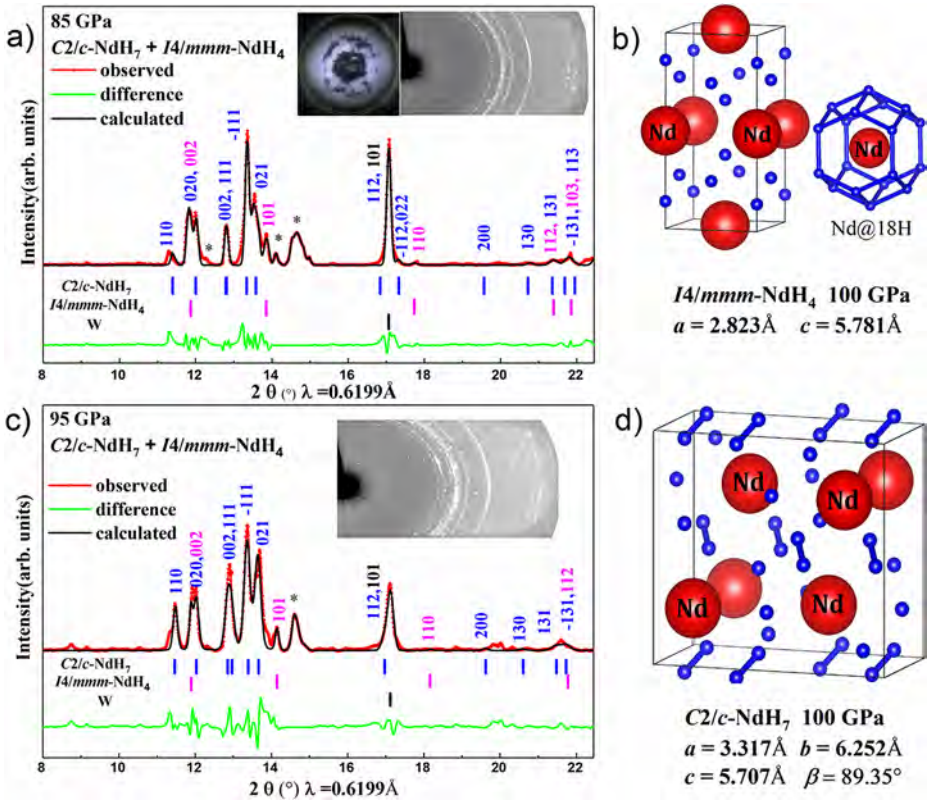


**Figure 2.** Experimental X-ray diffraction (XRD) patterns and Le Bail refinement of $I4/mmm$-$NdH_4$ and $C2/c$-$NdH_7$ at (a) 85 GPa and (c) 95 GPa. The experimental data and model fit for the structure are shown in red and black, respectively; the residues are indicated in green, while the unexplained peaks are marked by asterisks. The crystal structures of $I4/mmm$-$NdH_4$ and $C2/c$-$NdH_7$ at 100 GPa are shown in (b) and (d), respectively.

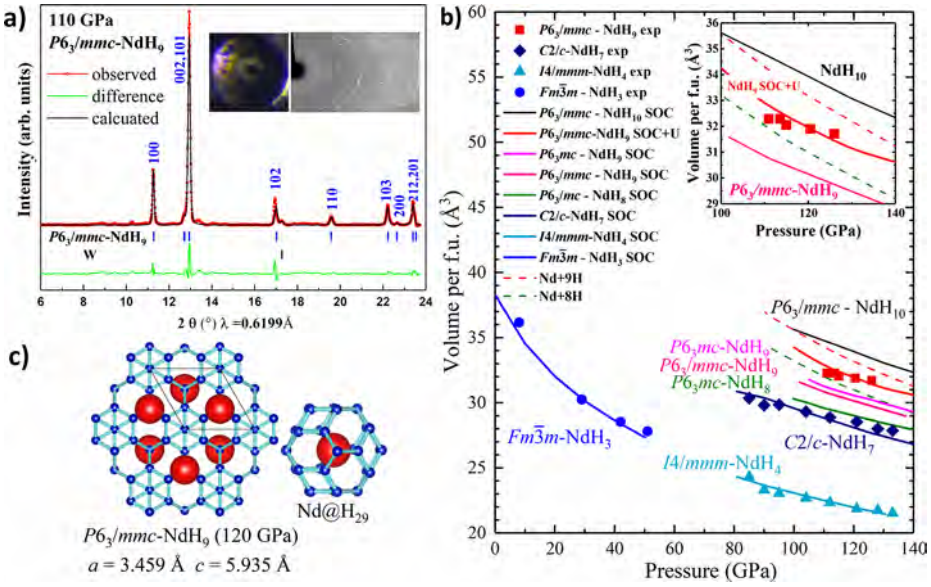


**Figure 3.** (a) Experimental XRD pattern and Le Bail refinement of $P6_3/mmc$-$NdH_9$. The experimental data and model fit for the structure are shown in red and black, respectively; the residues are indicated in green. (b) The equation of state of the synthesized Nd−H phases; theoretical results include spin−orbit coupling and magnetism. Inset: The distinction between $P6_3mc$-$NdH_8$, $P6_3/mmc$- and $P6_3mc$-$NdH_9$, and $P6_3/mmc$-$NdH_{10}$ phases. (c) The crystal structure of $P6_3/mmc$-$NdH_9$ and parameters of the unit cell.

corresponding pressure is 96 GPa. The rather complex diffraction pattern observed after laser heating shows that the reaction products are dominated by $C2/c$-$NdH_7$ with a small impurity of tetragonal $I4/mmm$-$NdH_4$ (Figures 2 and S1). Exploring this sample, we determined the experimental equation of state (EoS) of $C2/c$-$NdH_7$ and $I4/mmm$-$NdH_4$ in the pressure range from 85 to 135 GPa (Figure 3b) and found close agreement with the EoS obtained by DFT calculations.



https://dx.doi.org/10.1021/jacs.9b10439
J. Am. Chem. Soc. 2020, 142, 2803−2811

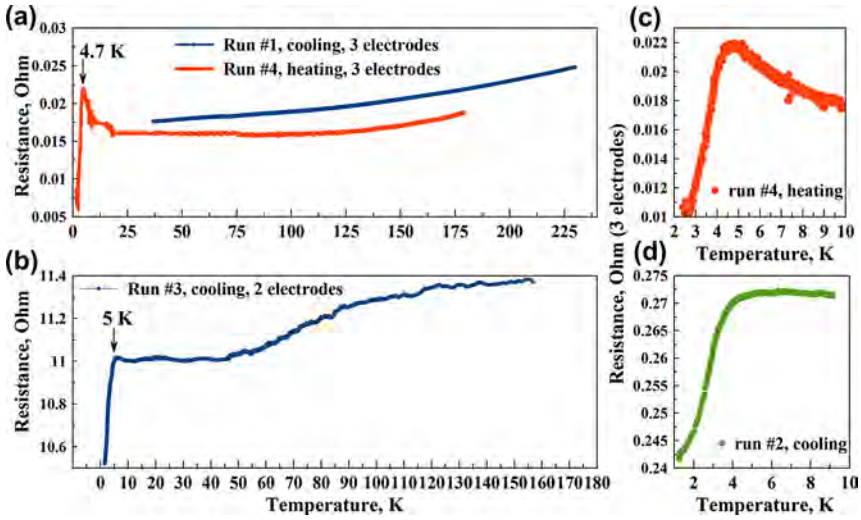


**Figure 4.** Dependence of electrical resistance of the synthesized sample on the temperature: (a, c, and d) in three-electrodes geometry; (b) in two-electrodes geometry. Runs 1−4 correspond to sequential steps of the laser heating.

In $I4/mmm$-$NdH_4$, which is isostructural to the recently found $I4/mmm$-$ThH_4$,[14,34] $CeH_4$,[17] and $CaH_4$,[35] the shortest H−H distance is $d_{min}$(H−H) = 1.55 Å at 100 GPa. Each Nd atom is bounded to 10 H atoms with $d$(Nd−H) = 2.02−2.08 Å. The hydrogen sublattice in $NdH_4$ is represented by the atomic hydrogen with a relatively high contribution of 1$s$-electrons to the electronic density of states $N(E_F)$. The experimental cell parameters of the discovered compounds are shown in Table S4. Fitting the experimental pressure−volume data in the pressure range from 85 to 135 GPa by the third-order Birch−Murnaghan equation of state gives $V_{100}$ = 45.7(2) Å$^3$, $K_{100}$ = 525(±15) GPa, and $K_{100}'$ = 2.7(±1.2).

The experimentally discovered $C2/c$-$NdH_7$ structure, which is close to the recently predicted $C2/m$-$AcH_8$[36] and $P2_1/m$-$ThH_7$,[34] at 100 GPa contains quasimolecular hydrogen $H_2$ units with $d$(H−H) = 0.92 Å. The remaining hydrogen (~30%) is in the atomic form. Each Nd atom is bounded to 17 H atoms with $d$(Nd−H) = 1.98−2.06 Å. The experimental cell parameters of this phase are shown in Table S5. Fitting the experimental pressure−volume data in the pressure range from 85 to 135 GPa by the third-order Birch−Murnaghan equation of state gives $V_{100}$ = 118.3(1) Å$^3$, $K_{100}$ = 522(±23) GPa and $K_{100}'$ = 2.4(±1.5).

**Synthesis of Superhydride $P6_3/mmc$-$NdH_9$.** The synthesis of higher neodymium hydrides was performed in a Z2 diamond anvil cell with Nd particle compressed in the $NH_3BH_3$ medium to 113 GPa and heated to 1800 K. The Raman signal of $H_2$ was detected at 4142.9 cm$^{-1}$, and the corresponding pressure is 115 GPa. The obtained diffraction pattern (Figure 3a, Figure S2b, and Table S6) corresponds to hexagonal $P6_3/mmc$-$NdH_9$, the structure of which is very close to the previously described hexagonal $P6_3/mmc$-$ThH_9$,[14] $UH_9$,[15] and $PrH_9$[18] (Figure 3c). Both known theoretical investigations of the high-pressure chemistry of the Nd−H system[13,25] claim the existence of cubic $NdH_8$ and $NdH_9$, while the experiment shows the presence of only one unexpected hexagonal $P6_3/mmc$-$NdH_9$ phase.

The calculated volumes of the ideal $P6_3/mmc$-$NdH_9$ structure are close to the experimental values, although the theoretical cell parameters have some deviations from the observed ones, for instance: $a$(exp) = 3.639 Å, $a$(theory) = 3.459 Å, $c$(exp) = 5.560 Å, and $c$(theory) = 5.935 Å at 120 GPa. These deviations, as well as the stability of hexagonal $NdH_9$, can be almost completely explained by DFT+$U$ approach with $U-J$ = 5 eV, chosen by using linear-response calculations (inset in Figure 3b; see the Supporting Information for details) and introduced for describing correlation effects. Note that such values of $U-J$ are commonly used for modeling $f$-electrons in Nd.[37−41] Additional ab initio studies show that the $P6_3/mmc$-$NdH_9$ structure is dynamically stable (Figure S5).

Because of the visible difference in cell parameters, we also considered the possible presence of additional hydrogen in the structure: $NdH_{9+x}$ ($x$ = 0−0.5), where the degree of nonstoichiometry ($x$) was determined by a linear interpolation of the dependence of the cell volume on the H content between 9 and 10 H atoms per Nd atom. In addition, we investigated $P6_3mc$-$NdH_8$ and $P6_3/mmc$-$NdH_{10}$ structures as possible candidates. $NdH_8$ is similar to predicted $P6_3mc$-$PrH_8$ and dynamically stable, lying on the convex hull at 100 GPa (Figure 3b). However, its predicted volume $V_{120}(NdH_8)$ = 29.04 Å$^3$ is much smaller than the experimental value of 31.88 Å$^3$. The proposed $P6_3/mmc$-$NdH_{10}$ is thermodynamically and dynamically unstable, and its predicted cell volume differs significantly from the measured one (Figure 3b).

$NdH_9$ has the same hexagonal structure as the whole family of reported hexagonal superhydrides: $YH_9$, $CeH_9$, $PrH_9$, and $ThH_9$. In $P6_3/mmc$-$NdH_9$, $H_{29}$ cages have the nearest H−H distance of 1.272 Å, the longest among all previously studied lanthanoid polyhydrides at 120 GPa, while the nearest Nd−H distance at this pressure is 1.973 Å. The experimental cell parameters of the compound are listed in Table S6. Fitting the experimental pressure−volume data in the range from 110 to 126 GPa using the third Birch−Murnaghan equation of state with fixed $K_{100}'$ = 4 gives $V_{100}$ = 32.8(1) Å$^3$ and $K_{100}$ = 719(±41) GPa.

After the destruction of diamonds in the Z2 DAC, followed by decompression from 106 to 51 GPa, the recorded XRD patterns demonstrated the presence of only one hydride phase: the metallic and magnetic $Fm\bar{3}m$-$NdH_3$ (Figure S2c) with the experimental cell parameter $a$ = 4.814 Å at 50 GPa, in agreement with the earlier predictions.[13] Fitting the experimental pressure−volume data for this phase in the pressure range from 7 to 50 GPa using the third-order Birch−


https://dx.doi.org/10.1021/jacs.9b10439
J. Am. Chem. Soc. 2020, 142, 2803−2811

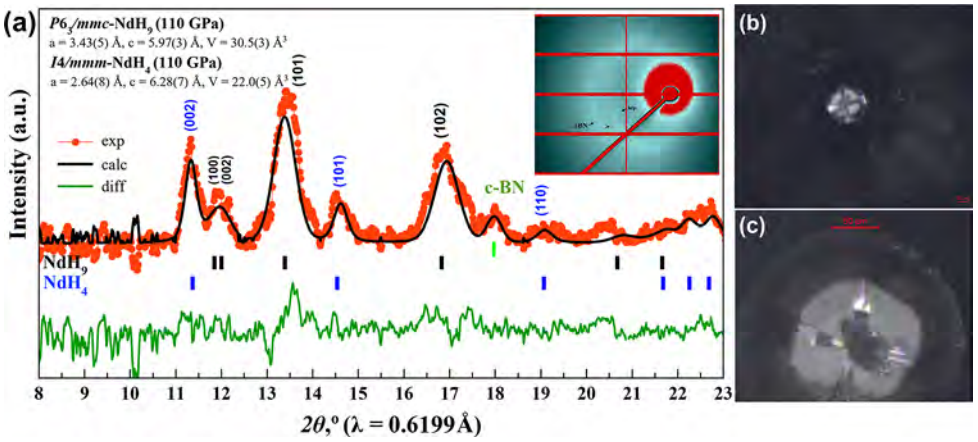


**Figure 5.** (a) X-ray diffraction pattern and Le Bail refinement of the $NdH_9$ and $NdH_4$ structures found in the electrical cell at 110 GPa. Reflection from *c*-BN ($a$ = 3.441 Å) corresponds to ~75 GPa; (b,c) optical microscopy of the culet of four-electrodes electrical cell and sample after laser heating.

Murnaghan equation of state gives $V_0$ = 42.3(3) Å$^3$, $K_0$ = 48.4(9) GPa, and $K_0'$ = 4.5(0).

**Measurements of the Electrical Resistance of *P6₃/mmc*-$NdH_9$.** The study of possible superconductivity in neodymium polyhydrides was performed in a Z3 cell with four 500 nm thick molybdenum electrodes prepared by magnetron sputtering ($E$ = 200 V) and UV lithography on a diamond culet of 80 $\mu$m in diameter. The cell was loaded with a 30 $\mu$m particle of Nd and ammonium borane layer (thickness ~15−20 $\mu$m) and then compressed to a pressure of 110 GPa using *c*-BN/epoxy insulating gasket. After pulsed laser heating of the sample during 3 s (total of 4 runs) over 1600 K and subsequent cooling in a cryostat, the electrode system was partially damaged, and several electrodes sequentially lost contact with the sample. In these cases, three-electrode (pseudo van der Pauw) and two-electrode schemes were used (Figure 4). As a result of the resistance ($R$) measurements in the range of 1.6−230 K, we have detected a sharp reproducible drop of $R(T)$ at 4.5 ± 0.5 K, possibly caused by the superconducting transition in $NdH_9$. At the same time, no clear and reproducible transitions or resistance drops were detected above 5 K.

To study the phase composition of the synthesized sample in the electrical cell, X-ray diffraction was performed using Beijing Synchrotron Research Facilities (BSRF, China). The wavelength of the synchrotron radiation was $\lambda$ = 0.6199 Å, with an exposure time of 10 min and a beam diameter of ~50 $\mu$m. Because of the presence of the electrodes, beam widening, and its weak intensity, the X-ray diffraction pattern cannot be quantitatively interpreted; however, the obtained diffractogram (Figure 5) qualitatively corresponds to a distorted hexagonal $P6_3/mmc$-$NdH_{9-x}$ mixed with tetragonal $I4/mmm$-$NdH_4$, the volume of which is close to the predicted value.

**Magnetic Properties of Neodymium Hydrides.** Ab initio calculations show that $P6_3/mmc$-$NdH_9$ exhibits metallic properties and magnetism (Figure S6). The contribution of hydrogen atoms to $N(E_F)$ is very low: 7.44 eV$^{-1}$ f.u.$^{-1}$ (97%) comes from Nd, while hydrogen gives only 0.22 eV$^{-1}$ f.u.$^{-1}$ (3%) at 120 GPa. It is expected that such a high electron density at the Fermi level drives an instability against spontaneous magnetization (see Stoner criterion[42]). Despite a clear analogy between Nd−H and Pr−H[18] systems (hexagonal $XH_9$ and tetragonal $XH_4$ polyhydrides), there is a significant difference in magnetic properties associated with the number of f-electrons. All Nd−H phases demonstrate strong magnetic properties (Figure 6a and b), more pronounced than

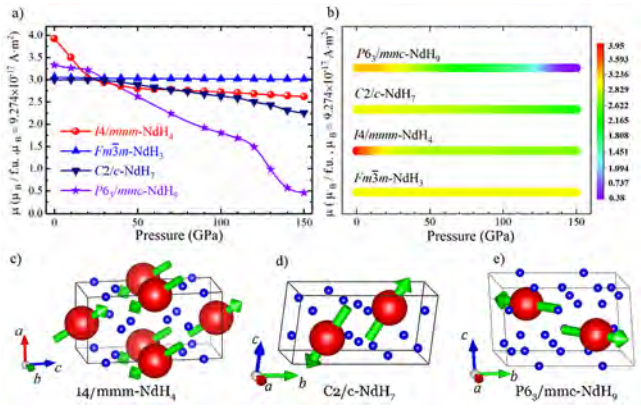


**Figure 6.** Magnetic properties of Nd−H compounds. Magnetism of Nd hydrides at pressures up to 150 GPa. (a) Magnetic moments (per Nd atom) at various pressures and (b) magnetic map of the Nd−H system as a function of pressure. Computed spin configurations for the 2 × 2 × 1 supercell of $NdH_4$ (c) and unit cells of $NdH_7$ (d) and $NdH_9$ (e). Arrows indicate magnetic moment directions on the Nd-atoms.

those of the corresponding praseodymium hydrides, except recently discovered $I4/mmm$-$PrH_4$,[43] which also possesses AFM ordering at 100 GPa (see Tables S8 and S9). This, probably, excludes the possibility of a classical s-wave superconductivity due to the large exchange spin-splitting in electron band structure (>450 meV). On the other hand, the coexistence of magnetism and a relatively strong electron−phonon interaction leaves open the possibility for more complex mechanisms of superconductivity as found, for example, in cuprates and Fe-containing pnictides.[24,44]

Simple spin-polarized calculations show that $NdH_7$ and $NdH_4$ maintain the magnetic moment of ~2.5−3.5 $\mu_B$ per Nd atom at low pressures, then start to slowly lose magnetism as pressure increases, while cubic $NdH_3$ keeps an almost constant magnetic moment, around 3 $\mu_B$ per Nd atom in the pressure range from 0 to 150 GPa. The magnetization of $NdH_9$ rapidly


https://dx.doi.org/10.1021/jacs.9b10439
J. Am. Chem. Soc. 2020, 142, 2803−2811

decreases with rising pressure and vanishes at ∼230 GPa (Figure 6a,b).

To understand the exact spin configurations at finite pressure, we have employed 10 different spin configurations using single-unit cells for $NdH_7$ and $NdH_9$, and 13 spin configurations and a 2 × 2 × 1 supercell for $NdH_4$. Using noncollinear calculations, the magnetic anisotropy energy (MAE) for Nd−H phases along different directions has been computed. Each magnetic configuration has been calculated at fixed lattice parameters and corresponding pressure. The results summarized in Table S8 clearly indicate the antiferromagnetic (AFM) character of $NdH_4$, $NdH_7$, and $NdH_9$ compounds (Figure 4c−e and Tables S8 and S9).

We have identified that $NdH_4$, $NdH_7$, and $NdH_9$ compounds possess AFM collinear [112], [144], and [23$\bar{1}$] orders, respectively. The Néel temperature can be estimated using the mean-field approximation $T_N^{MF} = \sum_{i,j} \frac{J_{i,j}S^2}{3k_B} \approx \min \frac{|E_{FM} - E_{AFM}|}{6k_B}$ as ∼5 K ($NdH_4$), ∼251 K ($NdH_7$), and ∼136 K ($NdH_9$). As it will be demonstrated below, the Néel temperatures are significantly higher than the expected superconducting $T_C$.

**Electron−Phonon Interaction in Neodymium Hydrides.** The study of the electron−phonon (el−ph) interaction and superconducting properties of neodymium hydrides is complicated because of two reasons: (1) possible interplay between magnetic ordering and el−ph interaction (see below) for which there is no relevant theory at this moment,[24,44] and (2) complex structure of the electronic density of states $N(E)$ (or DOS) with multiple van Hove singularities (vHs) near the Fermi level (Figures S6 and S11) caused by *f*-electrons of Nd. The latter makes us go beyond the commonly accepted "constant DOS approximation"[45] in calculations of the critical temperature and take into account the exact structure of the electronic density of states.

One of the consequences of the described effect is a strong dependence of the parameters of el−ph interaction on the Gaussian broadening ($\sigma$) parameter used in Quantum ESPRESSO (QE) (see the Supporting Information).[46] A similar situation was previously observed for praseodymium superhydrides $P6_3/mmc$-$PrH_9$ and $F\bar{4}3m$-$PrH_9$,[18] where the results of QE calculations are strongly dependent on $\sigma$ and on the chosen Pr pseudopotential.

To solve this problem, we applied a method developed by Lie and Carbotte[47] and analyzed the solution of the linearized Eliashberg equations,[48] taking into account the detailed structure of $N(E)$. As it was shown,[47] the $N(E)$ affects the Eliashberg equations via the following integral1:

$$\bar{N}(|\overline{\omega_i}|) = \frac{1}{\pi} \int_{\infty}^{-\infty} \frac{|\overline{\omega_i}|}{E^2 + |\overline{\omega_i}|^2} \frac{N(E)}{N(0)} \, dE \quad (1)$$

the contribution of which is determined by the $E \approx 0$ (=$E_F$) region in $N(E)$. To illustrate this, we calculated this expression for the studied compounds: $NdH_4$, $NdH_7$, and $NdH_9$ (Figure S11). Our results show that the maximum positive influence of $N(E)$ on $T_C$ is for $NdH_7$ and $NdH_9$, while for $NdH_4$ this effect is negative.

Harmonic calculations (for now neglecting magnetism) with using numerical solution of the isotropic set of Eliashberg equations and $\sigma$ = 0.025 Ry (which gives good convergence) show that $NdH_9$ at 120 GPa has quite a small electron−phonon coupling constant $\lambda$ = 0.43 and logarithmic average phonon frequency $\omega_{log}$ = 602 K. Contribution of the hydrogen sublattice to the DOS is very small (1−3%); that is why the matrix elements of the el−ph interaction are ∼0. As it is shown in Figure S11, accounting for the exact $N(E)$ structure leads to the increase of critical temperature. Calculations within the "constant DOS approximation"[45] led to a 10% lower $T_C$ = 3.7 K ($\mu^*$ = 0.1).

Combining the results of the VASP calculations with those of QE, we have obtained a more reliable Eliashberg function (Figure S13) to describe the electron−phonon interaction in $NdH_9$ (see the Supporting Information). This $\alpha^2F(\omega)$ leads to much higher $\lambda$ = 2.82 and lower $\omega_{log}$ = 272 K. The resulting critical temperature is 63 K ($\mu^*$ = 0.1) according to the Allen−Dynes formula.[49] However, consideration of antiferromagnetic ordering and spin-splitting leads to an almost complete suppression of superconductivity (see calculations with UppSC code).

The electron−phonon interaction in the molecular *C*2/*c*-$NdH_7$ at 100 GPa is even weaker than that in $NdH_9$: $\lambda$ = 0.23, $\omega_{log}$ = 842 K, and formal $T_C$ ($\mu^*$ = 0.1) is ∼0.01 K. This may be associated with the almost zero (∼1%) contribution to $N(E_F)$ from hydrogen (Figure S6b). Numerical solution of Eliashberg equations with accounting for the exact DOS structure at formal $\mu^*$ = 0 leads to a maximum possible $T_C$ of 2.7 K, while within the "constant DOS approximation"[45] we obtained a much lower value of 1.2 K.

Unexpectedly, a pronounced electron−phonon coupling is predicted for $I4/mmm$-$NdH_4$ (Figures S10 and S11). At 100 GPa, this compound has $\lambda$ = 0.54, $\omega_{log}$ = 857 K that corresponds to $T_C$ = 13.3 K ($\mu^*$ = 0.1). Because of the presence of a clear maximum of $N(E)$ close to $E_F$, the determination of superconducting $T_C$ strongly depends on the chosen $\sigma$-smoothing (Figures S10 and S11). This has a negative effect on $T_C$, and within the "constant DOS approximation"[45] the critical temperature is 15.2 K.

**Eliashberg Calculations with UppSC Code.** In conventional superconductors, Cooper pairs are formed from electrons in time-reversed states, and the relevant order parameter is proportional to the anomalous average $\langle c_{k\uparrow}c_{-k\downarrow}\rangle$. Because of the opposite spin of the paired electrons, an applied magnetic field tends to break the Cooper pair apart, and eventually at some critical field the superconducting state will be destroyed. In magnetic superconductors due to the underlying magnetic state, electrons feel such an effective magnetic field, which has a detrimental influence on the superconducting state.[50] This effective magnetic field lifts the spin degeneracy, therefore inducing a spin-splitting "gap" in the electron energy dispersion. Electrons at the Fermi level now need to overcome this energy to form spin singlet Cooper pairs.

To consider the possible effect of the magnetic structure on the electron−phonon interaction in $P6_3/mmc$-$NdH_9$, we analyzed the spin-resolved electronic band structure (Figure S6) and computed solutions of the Eliashberg equations using the UppSC code (see the Supporting Information). We found that the value of the spin-splitting at the Fermi level is too large (450 meV with $U-J$ = 0, and 890 meV at $U-J$ = 5 eV) for any finite superconducting solution, as confirmed by our calculations, which yield $T_C$ = 0 K even for $\mu^*$ = 0. Given that experiments find $T_C \approx$ 4.5 K, it is worthwhile to discuss possible scenarios. Aside from the potential presence of superconducting impurities (Mo,Nd)$C_xH_y$ or magnetic transitions, it is possible that, within our current calculations, we


https://dx.doi.org/10.1021/jacs.9b10439
J. Am. Chem. Soc. 2020, 142, 2803−2811

overestimated the spin-splitting ($h$) around the Fermi level. To investigate this scenario, we solved the Eliashberg equations for several values of $h$, $T$, and $\mu^*$. We found that for $\mu^* = 0.1$ and $h = 20$ meV, $T_C \approx 5$ K in agreement with experiment. Therefore, it may be that high-pressure $NdH_9$ could in principle be the first example material of the hydride family where superconductivity and AFM coexist, but at low temperature. Such a coexistence is not a priori to be excluded as has been shown, for example, in the case of unconventional AF superconductors.[51] Another possible scenario is that the low-temperature superconducting state may involve some form of a spin triplet superconducting order parameter. A possible candidate could be an equal spin triplet state.[52] Further investigations toward such an exciting direction would require solving the fully anisotropic Eliashberg equations,[53] which goes beyond the scope of the present work.

## CONCLUSIONS

Following the remarkable discovery of $LaH_{10}$, here we synthesized three novel neodymium polyhydrides, $P6_3/mmc$-$NdH_9$, $C2/c$-$NdH_7$, and $I4/mmm$-$NdH_4$, through the in situ laser-assisted decomposition of $NH_3BH_3$ with the simultaneous absorption of the released hydrogen by metallic Nd. Hexagonal $NdH_9$ is the next member of the $P6_3/mmc$ family of La, Ce, Pr, Th, and U nonahydrides. For all of the synthesized phases, the equations of state and unit cell parameters are in satisfactory agreement with our DFT or DFT+$U$ ($U-J = 5$ eV) calculations. Preliminary measurements of the electrical resistance of $NdH_9/NdH_4$ sample point to a possible SC transition at 4.5 ± 0.5 K at 110 GPa and the absence of superconductivity above 5 K. Although $P6_3/mmc$-$NdH_9$ has the highest H-content, the large spin-splitting in the electron band structure (>450 meV) and antiferromagnetic ordering almost rule out classical s-wave superconductivity. Thus, the intensity of superconducting properties declines in the La−Ce−Pr−Nd series of superhydrides, while magnetic properties become more pronounced.

Theoretical calculations predict that all of the neodymium hydrides exhibit strong magnetism at pressures below 150 GPa and possess collinear antiferromagnetic order, similar to $I4/mmm$-$PrH_4$, examined as a reference. The critical Néel temperatures for the newly synthesized neodymium hydrides were estimated using the mean-field approximation to be about 5 K ($NdH_4$), 251 K ($NdH_7$), and 136 K ($NdH_9$).

## ASSOCIATED CONTENT

### Supporting Information

The Supporting Information is available free of charge at https://pubs.acs.org/doi/10.1021/jacs.9b10439.

Experimental methods, computational details, structural information, electron and phonon properties of neodymium hydrides, magnetic properties of neodymium and praseodymium hydrides, superconductivity in neodymium hydrides and additional references (PDF)

## AUTHOR INFORMATION


### Corresponding Authors

**Xiaoli Huang** − *State Key Laboratory of Superhard Materials, College of Physics, Jilin University, Changchun 130012, China;* orcid.org/0000-0001-9628-5618; Email: huangxiaoli@jlu.edu.cn

**Alexander G. Kvashnin** − *Skolkovo Institute of Science and Technology, Moscow 121205, Russia;* orcid.org/0000-0002-0718-6691; Email: a.kvashnin@skoltech.ru

**Artem R. Oganov** − *Skolkovo Institute of Science and Technology, Moscow 121205, Russia; International Center for Materials Discovery, Northwestern Polytechnical University, Xi'an 710072, China;* orcid.org/0000-0002-9315-1419; Email: a.oganov@skoltech.ru

**Tian Cui** − *School of Physical Science and Technology, Ningbo University, Ningbo 315211, China; State Key Laboratory of Superhard Materials, College of Physics, Jilin University, Changchun 130012, China;* orcid.org/0000-0002-9664-848X; Email: cuitian@jlu.edu.cn

### Authors

**Di Zhou** − *State Key Laboratory of Superhard Materials, College of Physics, Jilin University, Changchun 130012, China*

**Dmitrii V. Semenok** − *Skolkovo Institute of Science and Technology, Moscow 121205, Russia*

**Hui Xie** − *State Key Laboratory of Superhard Materials, College of Physics, Jilin University, Changchun 130012, China*

**Defang Duan** − *State Key Laboratory of Superhard Materials, College of Physics, Jilin University, Changchun 130012, China;* orcid.org/0000-0002-6878-1830

**Alex Aperis** − *Department of Physics and Astronomy, Uppsala University, Uppsala SE-75120, Sweden*

**Peter M. Oppeneer** − *Department of Physics and Astronomy, Uppsala University, Uppsala SE-75120, Sweden*

**Michele Galasso** − *Skolkovo Institute of Science and Technology, Moscow 121205, Russia*

**Alexey I. Kartsev** − *Computing Center of Far Eastern Branch of the Russian Academy of Sciences (CC FEB RAS), Khabarovsk 680000, Russian Federation; School of Mathematics and Physics, Queen's University Belfast, Belfast, Northern Ireland BT7 1NN, United Kingdom;* orcid.org/0000-0002-3916-3443

Complete contact information is available at: https://pubs.acs.org/10.1021/jacs.9b10439


### Notes

The authors declare no competing financial interest.

## ACKNOWLEDGMENTS

We thank the staff of the Shanghai and Beijing Synchrotron Radiation Facility. We express our gratitude to Bingbing Liu's group (Jilin University) for their help in the laser heating of samples. This work was supported by the National Key R&D Program of China (Grant no. 2018YFA0305900), the National Natural Science Foundation of China (Grant nos. 11974133, 51720105007, 51632002, 11674122, 11574112, 11474127, and 11634004), the National Key Research and Development Program of China (Grant no. 2016YFB0201204), the Program for Changjiang Scholars and Innovative Research Team in University (Grant no. IRT_15R23), and the National Fund for Fostering Talents of Basic Science (Grant no. J1103202). A.R.O. thanks the Russian Science Foundation (Grant no. 19-72-30043). A.G.K., D.V.S., and A.I.K. thank the Russian Foundation for Basic Research (Grant nos. 19-03-00100 and 18-29-11051 mk). A.A. and P.M.O. acknowledge support from the Swedish Research Council (VR), from the Röntgen-Ångström cluster, and from the Swedish National Infrastructure for Computing (SNIC). We thank Professor R. Akashi (University of Tokyo) for valuable discussions on the

influence of precise density of states on critical temperature of superconductivity.

## REFERENCES


(1) Ashcroft, N. W. Metallic Hydrogen: A High-Temperature Superconductor? *Phys. Rev. Lett.* **1968**, *21* (26), 1748−1749.

(2) McMahon, J. M.; Ceperley, D. M. High-temperature superconductivity in atomic metallic hydrogen. *Phys. Rev. B: Condens. Matter Mater. Phys.* **2011**, *84*, 144515.

(3) Borinaga, M.; Errea, I.; Calandra, M.; Mauri, F.; Bergara, A. Anharmonic effects in atomic hydrogen: Superconductivity and lattice dynamical stability. *Phys. Rev. B: Condens. Matter Mater. Phys.* **2016**, *93* (17), 174308.

(4) McMahon, J. M.; Morales, M. A.; Pierleoni, C.; Ceperley, D. M. The properties of hydrogen and helium under extreme conditions. *Rev. Mod. Phys.* **2012**, *84* (4), 1607−1653.

(5) Azadi, S.; Monserrat, B.; Foulkes, W. M.; Needs, R. J. Dissociation of high-pressure solid molecular hydrogen: a quantum Monte Carlo and anharmonic vibrational study. *Phys. Rev. Lett.* **2014**, *112* (16), 165501.

(6) McMinis, J.; III, R. C. C.; Lee, D.; Morales, M. A. Molecular to Atomic Phase Transition in Hydrogen under High Pressure. *Phys. Rev. Lett.* **2015**, *114*, 105305.

(7) Ashcroft, N. W. Hydrogen dominant metallic alloys: high temperature superconductors? *Phys. Rev. Lett.* **2004**, *92* (18), 187002−1−187002−4.

(8) Drozdov, A. P.; Eremets, M. I.; Troyan, I. A.; Ksenofontov, V.; Shylin, S. I. Conventional superconductivity at 203 K at high pressures in the sulfur hydride system. *Nature* **2015**, *525* (7567), 73−6.

(9) Somayazulu, M.; Ahart, M.; Mishra, A. K.; Geballe, Z. M.; Baldini, M.; Meng, Y.; Struzhkin, V. V.; Hemley, R. J. Evidence for Superconductivity above 260 K in Lanthanum Superhydride. *Phys. Rev. Lett.* **2019**, *122*, 027001.

(10) Drozdov, A. P.; Kong, P. P.; Minkov, V. S.; Besedin, S. P.; Kuzovnikov, M. A.; Mozaffari, S.; Balicas, L.; Balakirev, F. F.; Graf, D. E.; Prakapenka, V. B.; Greenberg, E.; Knyazev, D. A.; Tkacz, M.; Eremets, M. I. Superconductivity at 250 K in lanthanum hydride under high pressures. *Nature* **2019**, *569* (7757), 528−531.

(11) Goncharov, A. F.; Beck, P.; Struzhkin, V. V.; Hemley, R. J.; Crowhurst, J. C. Laser-heating diamond anvil cell studies of simple molecular systems at high pressures and temperatures. *J. Phys. Chem. Solids* **2008**, *69* (9), 2217−2222.

(12) Geballe, Z. M.; Liu, H.; Mishra, A. K.; Ahart, M.; Somayazulu, M.; Meng, Y.; Baldini, M.; Hemley, R. J. Synthesis and Stability of Lanthanum Superhydrides. *Angew. Chem., Int. Ed.* **2018**, *129*, 6.

(13) Peng, F.; Sun, Y.; Pickard, C. J.; Needs, R. J.; Wu, Q.; Ma, Y. Hydrogen Clathrate Structures in Rare Earth Hydrides at High Pressures: Possible Route to Room-Temperature Superconductivity. *Phys. Rev. Lett.* **2017**, *119* (10), 107001.

(14) Semenok, D. V.; Kvashnin, A. G.; Ivanova, A. G.; Svitlyk, V.; Fominski, V. Y.; Sadakov, A. V.; Sobolevskiy, O. A.; Pudalov, V. M.; Troyan, I. A.; Oganov, A. R. Superconductivity at 161 K in thorium hydride $ThH_{10}$: Synthesis and properties. *Mater. Today* **2019**, DOI: 10.1016/j.mattod.2019.10.005.

(15) Kruglov, I. A.; Kvashnin, A. G.; Goncharov, A. F.; Oganov, A. R.; Lobanov, S. S.; Holtgrewe, N.; Jiang, S. Q.; Prakapenka, V. B.; Greenberg, E.; Yanilkin, A. V. Uranium polyhydrides at moderate pressuresPredict: Prediction, synthesis, and expected superconductivity. *Sci. Adv.* **2018**, *4*, eaat9776.

(16) Salke, N. P.; Esfahani, M. M. D.; Zhang, Y.; Kruglov, I. A.; Zhou, J.; Wang, Y.; Greenberg, E.; Prakapenka, V. B.; Liu, J.; Oganov, A. R.; Lin, J.-F. Synthesis of clathrate cerium superhydride $CeH_9$ at 80 GPa with anomalously short H-H distance. *Nat. Commun.* **2019**, *10*, 4453.

(17) Li, X.; Huang, X.; Duan, D.; Pickard, C. J.; Zhou, D.; Xie, H.; Zhuang, Q.; Huang, Y.; Zhou, Q.; Liu, B.; Cui, T. Polyhydride $CeH_9$ with an atomic-like hydrogen clathrate structure. *Nat. Commun.* **2019**, *10*, 3461.

(18) Zhou, D.; Semenok, D. V.; Duan, D.; Xie, H.; Huang, X.; Chen, W.; Li, X.; Liu, B.; Oganov, A. R.; Cui, T. Superconducting Praseodymium Superhydrides. *Sci. Adv.* **2020**, DOI: 10.1126/sciadv.aax6849.

(19) Pépin, C.; Loubeyre, P.; Occelli, F.; Duma, P. Synthesis of lithium polyhydrides above 130 GPa at 300 K. *Proc. Natl. Acad. Sci. U. S. A.* **2015**, *112* (25), 7673−7676.

(20) Struzhkin, V. V.; Kim, D. Y.; Stavrou, E.; Muramatsu, T.; Mao, H. K.; Pickard, C. J.; Needs, R. J.; Prakapenka, V. B.; Goncharov, A. F. Synthesis of sodium polyhydrides at high pressures. *Nat. Commun.* **2016**, *7*, 12267.

(21) Feng, X.; Zhang, J.; Gao, G.; Liu, H.; Wang, H. Compressed Sodalite-like MgH6 as a Potential High-temperature Superconductor. *RSC Adv.* **2015**, *5* (73), 59292−59296.

(22) Wang, H.; Tse, J. S.; Tanaka, K.; Iitaka, T.; Ma, Y. Superconductive sodalite-like clathrate calcium hydride at high pressures. *Proc. Natl. Acad. Sci. U. S. A.* **2012**, *109* (17), 6463−6466.

(23) Liu, H.; Naumov, I. I.; Hoffmann, R.; Ashcroft, N. W.; Hemley, R. J. Potential high-Tc superconducting lanthanum and yttrium hydrides at high pressure. *Proc. Natl. Acad. Sci. U. S. A.* **2017**, *114* (27), 5.

(24) Keimer, B.; Kivelson, S. A.; Norman, M. R.; Uchida, S.; Zaanen, J. From quantum matter to high-temperature superconductivity in copper oxides. *Nature* **2015**, *518* (7538), 179−86.

(25) Semenok, D. V.; Kruglov, I. A.; Kvashnin, A. G.; Oganov, A. R. On Distribution of Superconductivity in Metal Hydrides; arXiv:1806.00865, 2018.

(26) Chesnut, G. N.; Vohra, Y. K. a-uranium phase in compressed neodymium metal. *Phys. Rev. B: Condens. Matter Mater. Phys.* **2000**, *61*, R3768−R3771.

(27) Vajda, P.; Daou, J. N. Rare Earths-Hydrogen. *Solid State Phenom.* **1996**, *49*−*50*, 71−158.

(28) Oganov, A. R.; Glass, C. W. Crystal structure prediction using ab initio evolutionary techniques: Principles and applications. *J. Chem. Phys.* **2006**, *124*, 244704.

(29) Oganov, A. R.; Lyakhov, R. O.; Valle, M. How Evolutionary Crystal Structure Prediction Works-and Why. *Acc. Chem. Res.* **2011**, *44*, 227−237.

(30) Lyakhov, A. O.; Oganov, A. R.; Stokes, H. T.; Zhu, Q. New developments in evolutionary structure prediction algorithm USPEX. *Comput. Phys. Commun.* **2013**, *184* (4), 1172−1182.

(31) Chellappa, R. S.; Somayazulu, M.; Struzhkin, V. V.; Autrey, T.; Hemley, R. J. Pressure-induced complexation of $NH_3BH_3$−$H_2$. *J. Chem. Phys.* **2009**, *131*, 224515.

(32) Song, Y. New perspectives on potential hydrogen storage materials using high pressure. *Phys. Chem. Chem. Phys.* **2013**, *15* (35), 14524−47.

(33) Potter, R. G.; Somayazulu, M.; Cody, G.; Hemley, R. J. High Pressure Equilibria of Dimethylamine Borane, Dihydridobis-(dimethylamine)boron(III) Tetrahydridoborate(III), and Hydrogen. *J. Phys. Chem. C* **2014**, *118* (14), 7280−7287.

(34) Kvashnin, A. G.; Semenok, D. V.; Kruglov, I. A.; Wrona, I. A.; Oganov, A. R. High-Temperature Superconductivity in Th-H System at Pressure Conditions. *ACS Appl. Mater. Interfaces* **2018**, *10*, 43809−43816.

(35) Wu, G.; Huang, X.; Xie, H.; Li, X.; Liu, M.; Liang, Y.; Huang, Y.; Duan, D.; Li, F.; Liu, B.; Cui, T. Unexpected calcium polyhydride CaH4: A possible route to dissociation of hydrogen molecules. *J. Chem. Phys.* **2019**, *150*, 044507.

(36) Semenok, D. V.; Kvashnin, A. G.; Kruglov, I. A.; Oganov, A. R. Actinium Hydrides $AcH_{10}$, $AcH_{12}$, and $AcH_{16}$ as High-Temperature Conventional Superconductors. *J. Phys. Chem. Lett.* **2018**, *9* (8), 1920−1926.

(37) Zaari, H.; Boujnah, M.; El hachimi, A. G.; Benyoussef, A.; El Kenz, A. Electronic structure and X-ray magnetic circular dichroic of Neodymium doped ZnTe using the GGA + U approximation. *Comput. Mater. Sci.* **2014**, *93*, 91−96.

(38) Reshak, A. H.; Piasecki, M.; Auluck, S.; Kityk, I. V.; Khenata, R.; Andriyevsky, B.; Cobet, C.; Esser, N.; Majchrowski, A.;




https://dx.doi.org/10.1021/jacs.9b10439
J. Am. Chem. Soc. 2020, 142, 2803−2811

Swirkowicz, M.; Diduszko, R.; Szyrski, W. Effect of U on the Electronic Properties of Neodymium Gallate (NdGaO3): Theoretical and Experimental Studies. *J. Phys. Chem. B* **2009**, *113*, 15237−15242.
(39) Shankar, A.; Rai, D. P.; Thapa, R. K. Structural, electronic, magnetic and optical properties of neodymium chalcogenides using LSDA+Umethod. *J. Semicond.* **2012**, *33* (8), 082001.
(40) Kozub, A. L.; Shick, A. B.; Máca, F.; Kolorenč, J.; Lichtenstein, A. I. Electronic structure and magnetism of samarium and neodymium adatoms on free-standing graphene. *Phys. Rev. B: Condens. Matter Mater. Phys.* **2016**, *94*, 12.
(41) Morice, C.; Artacho, E.; Dutton, S. E.; Kim, H. J.; Saxena, S. S. Electronic and magnetic properties of superconducting $LnO_{1-x}F_xBiS_2$ (Ln = La, Ce, Pr, and Nd) from first principles. *J. Phys.: Condens. Matter* **2016**, *28* (34), 345504.
(42) Stoner, E. G. Collective Electron Ferromagnetism. *Proc. R. Soc.* **1938**, *A165*, 372.
(43) Peña-Alvarez, M.; Binns, J.; Hermann, A.; Kelsall, L. C.; Dalladay-Simpson, P.; Gregoryanz, E.; Howie, R. T. Praseodymium polyhydrides synthesized at high temperatures and pressures. *Phys. Rev. B: Condens. Matter Mater. Phys.* **2019**, *100*, 184109.
(44) Johnston, D. C. The puzzle of high temperature superconductivity in layered iron pnictides and chalcogenides. *Adv. Phys.* **2010**, *59* (6), 803−1061.
(45) Sano, W.; Koretsune, T.; Tadano, T.; Akashi, R.; Arita, R. Effect of Van Hove singularities on high-$T_C$ superconductivity in H3S. *Phys. Rev. B: Condens. Matter Mater. Phys.* **2019**, *93*, 094525.
(46) Giannozzi, P.; Baroni, S.; Bonini, N.; Calandra, M.; Car, R.; Cavazzoni, C.; Ceresoli, D.; Chiarotti, G. L.; Cococcioni, M.; Dabo, I.; Corso, A. D.; Gironcoli, S. d.; Fabris, S.; Fratesi, G.; Gebauer, R.; Gerstmann, U.; Gougoussis, C.; Kokalj, A.; Lazzeri, M.; Martin-Samos, L.; Marzari, N.; Mauri, F.; Mazzarello, R.; Paolini, S.; Pasquarello, A.; Paulatto, L.; Sbraccia, C.; Scandolo, S.; Sclauzero, G.; Seitsonen, A. P.; Smogunov, A.; Umari, P.; Wentzcovitch, R. M. QUANTUM ESPRESSO: a modular and open-source software project for quantum simulations of materials. *J. Phys.: Condens. Matter* **2009**, *21* (39), 395502.
(47) Lie, S. G.; Carbotte, J. P. Dependence of Tc on electronic density of states. *Solid State Commun.* **1978**, *26* (8), 511−514.
(48) Eliashberg, G. M. Interactions between Electrons and Lattice Vibrations in a Superconductor. *JETP* **1959**, *11*, 696−702.
(49) Allen, P. B.; Dynes, R. C. Transition temperature of strong-coupled superconductors reanalyzed. *Phys. Rev. B* **1975**, *12* (3), 905−922.
(50) Fulde, P.; Zwicknagl, G. Antiferromagnetic superconductors (invited). *J. Appl. Phys.* **1982**, *53* (11), 8064−8069.
(51) Aperis, A.; Varelogiannis, G.; Littlewood, P. B.; Simons, B. D. Coexistence of spin density wave, d-wave singlet and staggered $\pi$-triplet superconductivity - IOPscience. *J. Phys.: Condens. Matter* **2008**, *20* (43), 434235.
(52) Sigrist, M.; Ueda, K. Phenomenological theory of unconventional superconductivity. *Rev. Mod. Phys.* **1991**, *63*, 239.
(53) Aperis, A.; Maldonado, P.; Oppeneer, P. M. Ab initio theory of magnetic-field-induced odd-frequency two-band superconductivity in $MgB_2$. *Phys. Rev. B: Condens. Matter Mater. Phys.* **2015**, *92*, 054516.


https://dx.doi.org/10.1021/jacs.9b10439
*J. Am. Chem. Soc.* 2020, 142, 2803−2811